NATIONAL ADVISORY COMMITTEE FOR AERONAUTICS

WARTIME REPORT

ORIGINALLY ISSUED
February 1945 as
Advance Confidential Report L5B01

DETERMINATION OF THE EFFECT OF HORIZONTAL-TAIL FLEXIBILITY ON LONGITUDINAL CONTROL CHARACTERISTICS

By S. M. Harmon

Langley Memorial Aeronautical Laboratory
Langley Field, Va.

NACA

WASHINGTON

NACA ACR No. L5B01

NATIONAL ADVISORY COMMITTEE FOR AERONAUTICS

ADVANCE CONFIDENTIAL REPORT

DETERMINATION OF THE EFFECT OF HORIZONTAL-TAIL FLEXIBILITY ON LONGITUDINAL CONTROL CHARACTERISTICS

By S. M. Harmon

SUMMARY

An iteration method is given for determining the longitudinal control characteristics of a flexible horizontal tail. The method permits factors such as the actual spanwise variation of elasticity and the aerodynamic induction effects due to three-dimensional flow to be accounted for to any degree of accuracy appropriate to a particular case.

An analysis is included of the effects of horizontal-tail flexibility on the tail effectiveness, the hinge-moment characteristics, and the control-force gradients in a dive recovery for two modern fighter airplanes. The effects of variations in speed, altitude, elevator stiffness, and center-of-gravity movements are considered. The results of these calculations for speeds below that at which critical compressibility effects occur indicate for the two airplanes significant effects due to the tail flexibility. It appears that the location of the flexural axis of the stabilizer too far behind the aerodynamic center of the tail may cause excessive control forces in a dive recovery at high speeds.

INTRODUCTION

The design of tail structures for high-speed flight requires special consideration of the factors that

provide sufficient rigidity in torsion in order to ensure satisfactory control and maneuverability for the complete speed range. Reference 1 presents an analytical treatment of the effect of horizontal-tail flexibility on longitudinal control characteristics. The analysis of reference 1 is based essentially on the assumption of a semirigid tail structure having a linear spanwise twist distribution and on two-dimensional section force theory. The assumption of a semirigid tail, however, does not provide for the establishment of the required equilibrium between the aerodynamic and elastic forces at every section; consequently there is, in general, no assurance of the extent to which the arbitrarily chosen twist distribution represents the distortion of the actual flexible tail. In addition, the low aspect ratios commonly employed on tails produce significant induced effects on the aerodynamic forces. It appears, therefore, that more reliable predictions of the control characteristics of a flexible tail could be obtained by taking account of the actual spanwise variation of elasticity and of the aerodynamic induction effects.

The present paper presents a method for determining the control characteristics of a flexible tail that takes account of factors, such as the actual spanwise variation of elasticity and the aerodynamic induced effects, to a degree of accuracy appropriate to any particular case. The method is based on an iteration procedure in which the effect of the tail flexibility is obtained by means of a series formed by the addition of the incremental effects resulting from each iteration. The rapidity of the convergence of this series depends on the degree of rigidity of the tail, and the increments for the higher-order iterations can usually be estimated from a knowledge of the values obtained from the preceding iterations.

In order to illustrate the iteration procedure and to indicate the magnitude of the effects of tail flexibility in some typical cases, the present investigation includes an analysis for two modern fighter airplanes of the effect of horizontal-tail flexibility on the tail effectiveness, on the hinge-moment characteristics, and on the control-force gradients required in recovery from a dive. The results of these computations are given for sea level and for an altitude of 30,000 feet for a speed range corresponding to Mach numbers ranging from 0 to 0.72.

[redacted]

SYMBOLS

M	pitching-moment contribution of tail about center of gravity of airplane, positive when airplane noses up, foot-pounds; Mach number when used to account for compressibility effects
l_t	tail length, measured from center of gravity of airplane to elastic axis of tail, feet
e	distance from aerodynamic center to flexural center at a section for the tail, positive when aerodynamic center is ahead of flexural center, feet
ρ	air density, slugs per cubic foot
V	true airspeed, miles per hour
q	dynamic pressure, pounds per square foot $\left[(1.467)^2 \frac{\rho}{2} V^2\right]$
T	total torque of tail, positive when stabilizer leading edge tends to nose upward (the derivative $\frac{dT}{d\eta}$ represents the torque per unit span at a tail section), foot-pounds
c	wing chord, feet
b	span (of wing, unless otherwise indicated), feet
S	area (of wing unless otherwise indicated), square feet
$\bar{c}_e$	root-mean-square elevator chord, measured behind hinge line, feet
c_w	mean aerodynamic chord of wing, feet
y	coordinate indicating fixed position along span from center line
η	coordinate indicating variable position along span from center line

[redacted]

A	aspect ratio
A'	fictitious aspect ratio employed in corrections for compressibility effects $\left(A\sqrt{1-M^2}\right)$
E	ratio of semiperimeter of ellipse to span of airfoil surface, primed to indicate fictitious plan form employed in corrections for compressibility effects
a_{o_t}	two-dimensional lift-curve slope for tail
c_{l_t}	section lift coefficient for tail; primed to refer to section lift coefficient of a fictitious plan form employed in corrections for compressibility effects
a_{t_R}	geometric angle of attack of the tail, measured from zero-lift line at section for assumed rigid tail
θ	angular deflection of stabilizer due to tail flexibility, positive when leading edge moves upward, degrees
a_t	geometric angle of attack of tail, measured from zero-lift line at section for flexible tail, degrees $\left(a_{t_R} + \theta\right)$
δ_R	elevator deflection at section for assumed rigid tail, positive when trailing edge moves downward, degrees
ϕ	angular deflection of elevator section due to elevator flexibility, positive when trailing edge moves downward, degrees
δ	elevator deflection at section in flexible tail, degrees $(\delta_R + \phi - \theta)$
$\Delta\delta_R$	change in δ_R per unit change in normal acceleration in recovery from dive, degrees per g

[redacted]

Δa_{t_R} change in a_{t_R} per unit change in normal acceleration in recovery from dive, degrees per g

F_n change in elevator control force per unit change in normal acceleration, pounds per g

g acceleration of gravity, 32.2 feet per second^2

$\left(\frac{\partial a_{t_R}}{\partial \delta_R}\right)_{c_{l_t}}$ rate of change of section angle of attack with elevator deflection for constant lift at section for assumed rigid tail

$\left(\frac{\partial c_h}{\partial c_{l_t}}\right)_{\delta_R}$ rate of change of section hinge-moment coefficient with section lift coefficient for constant elevator deflection for assumed rigid tail

$\left(\frac{\partial c_h}{\partial \delta_R}\right)_{c_{l_t}}$ rate of change of section hinge-moment coefficient with section elevator deflection of assumed rigid tail in degrees for constant section lift

$\left(\frac{\partial c_m}{\partial \delta_R}\right)_{c_{l_t}}$ rate of change of section pitching-moment coefficient with section elevator deflection of assumed rigid tail in degrees for constant section lift

C_L airplane lift coefficient

a three-dimensional slope of lift curve for airplane

$\left(\frac{d\delta_R}{dC_L}\right)_R$ rate of change of elevator deflection with airplane lift coefficient for trim for assumed rigid tail, degrees

[redacted]

$d\epsilon/d\alpha_w$ rate of change of downwash angle at tail with wing angle of attack, degrees per degree

$\frac{1}{\sqrt{1 - M^2}}$ compressibility correction factor, where M = Mach number

B compressibility correction factor $\left(\frac{EA + 2}{E'A' + 2}\right)$

K_e elevator gearing ratio, as obtained with no load on tail, radians per foot

W airplane gross weight, pounds

H total hinge moment on elevator, positive when leading edge tends to move upward, foot-pounds

C_h elevator hinge-moment coefficient $\left(\frac{H}{q\bar{c}_e^2 b_e}\right)$

$\frac{\partial C_h}{\partial \delta_R}$ rate of change of C_h with δ_R as obtained for given movement of elevator control stick

$\frac{\partial C_h}{\partial \alpha_{t_R}}$ rate of change of C_h with α_{t_R} over tail

C_m pitching-moment coefficient due to tail about center of gravity of airplane (M/qSc_w)

$\frac{\partial C_m}{\partial \delta_R}$ rate of change of C_m with δ_R, as obtained for given movement of elevator control stick

$\frac{\partial C_m}{\partial \alpha_{t_R}}$ rate of change of C_m with α_{t_R} over tail

$\left(\frac{\partial \delta_R}{\partial \alpha_{t_R}}\right)_{C_m}$ rate of change of δ_R for given movement of elevator control stick with α_{t_R} over tail, with C_m constant $\left(\frac{-\partial C_m/\partial \alpha_{t_R}}{\partial C_m/\partial \delta_R}\right)$

[redacted]

$t(y)$ total torque transmitted by the stabilizer section at station y, foot-pounds

$$\left(\int_{y}^{b_t/2} \frac{dt}{d\eta}\, d\eta\right)$$

$h(y)$ total hinge moment transmitted by elevator section at station y, foot-pounds

$$\left(\int_{y}^{b_t/2} \frac{dh}{d\eta}\, d\eta\right)$$

$C_{TR_s}(\eta)$ coefficient of torsional rigidity for stabilizer at station η, equal to $\frac{t(\eta)}{d\theta/d\eta}$, where $d\theta/d\eta$ is the slope of the θ curve at station η, pound-feet^2 per degree

$C_{TR_e}(\eta)$ coefficient of torsional rigidity for elevator at station η, equal to $\frac{h(\eta)}{d\phi/d\eta}$, where $d\phi/d\eta$ is slope of ϕ curve at station η, pound-feet^2 per degree

$\frac{d\phi}{dH}$ rate of change of section elevator twist with total hinge moment on a loaded half of elevator surface as measured in static tests, degrees per foot-pound

Subscripts:

t	tail
w	wing
e	elevator
s	stabilizer
R	refers to assumed rigid tail
0, 1, 2, etc.	numerical subscripts used to indicate the order of twist iteration

PRESENTATION OF METHOD

Development of Formulas

The pitching moment due to the tail about the center of gravity of an airplane, considered positive in the nose-up condition, is given by the equation

$$M = \left(-l_t q \int_{-b_t/2}^{b_t/2} c_{l_t} c_t \, d\eta\right) + T \qquad (1)$$

where T is the tail pitching moment about the flexural axis of the tail, assumed to be positive when the leading edge tends to move upward. In conventional airplanes, the value of T usually increases the elevator effectiveness numerically by about 5 percent. If the lifting-line theory of reference 2 is followed, the lift coefficient c_{l_t} in equation (1) is given as a function of the spanwise coordinate y in the form

$$c_{l_t}(y) = a_o \left[a_t - \left(\frac{\partial a_{t_R}}{\partial \delta_R}\right)_{c_{l_t}} \delta - \frac{1}{\partial \pi} \int_{-b_t/2}^{b_t/2} \frac{\frac{dc_{l_t} c_t}{d\eta} d\eta}{y - \eta} \right] \qquad (2)$$

in which, for the flexible tail,

$$a_t = a_{t_R} + \theta$$

$$\delta = \delta_R + \phi - \theta$$

The integral expression in equation (2) represents the induced downwash angle. The determination of the lift distribution by means of the lifting-line theory for an arbitrary angle-of-attack and chord distribution has received much attention, and numerous methods (references 2, 3, and 4) are available for obtaining the solution of equation (2) when the functions a_t and δ are given.

The basic consideration in the determination of the spanwise twist distributions for the stabilizer and

[redacted]

elevator, $\theta(y)$ and $\phi(y)$, for use in equation (2) is the establishment, at every section, of equilibrium between the aerodynamic and the elastic forces acting on the tail structure. In the present analysis, θ and ϕ are determined on the basis of the theory of pure torsion of tubes (references 5 and 6). Other considerations relating to the torsional effects of the axial stresses induced by the restraints to the free warping of the sections of the stabilizer and elevator and to the effects of the bending of the ribs can be accounted for by employing the proper parameters and following the procedure of successive approximations or iterations described herein under "Iteration Method."

The aerodynamic twisting moment for a symmetrical airfoil section results from the lift distribution contributed by the angle of attack, which acts at the aerodynamic center of the section, and the lift distribution contributed by the elevator deflection, which acts at its center of pressure. If the section is unsymmetrical, the lift distribution due to camber contributes a further increment to the twisting moment. On the basis of the foregoing assumptions, if a symmetrical section is used, the applied twisting moment across a section $d\eta$ of the tail is

$$dT(\eta) = \left[\delta\left(\frac{\partial c_m}{\partial \delta_R}\right)_{c_{l_t}} + c_{l_t}\frac{e}{c_t}\right] q c_t^2 \, d\eta \qquad (3)$$

In order to obtain the torsional moment on the stabilizer, the moment acting about the elevator hinges should be deducted from the total twisting moment on the tail, because the elevator hinge moment is normally transmitted to the fuselage through the torque tube. The applied twisting moment across a section $d\eta$ of the stabilizer, therefore, is given by

$$dt(\eta) = dT(\eta) - dh(\eta) \qquad (4)$$

where $dh(\eta)$ is the elevator hinge moment at the section η of width $d\eta$ and

$$dh(\eta) = \left[\delta\left(\frac{\partial c_h}{\partial \delta_R}\right)_{c_{l_t}} + c_{l_t}\left(\frac{\partial c_h}{\partial c_{l_t}}\right)_{\delta_R}\right] q c_e^2 \, d\eta \qquad (5)$$

[redacted]

The expression for c_{l_t} in equations (3) and (5) is given in equation (2).

The total torque transmitted by a stabilizer section y is

$$t(y) = \int_y^{b_t/2} \frac{dt}{d\eta} d\eta \tag{6}$$

Division of equation (4) by $d\eta$ and substitution of the value obtained for $dt/d\eta$ in equation (6) gives

$$t(y) = \int_y^{b_t/2} \left(\frac{dT}{d\eta} - \frac{dh}{d\eta} \right) d\eta \tag{7}$$

where $\frac{dT}{d\eta}(\eta)$ and $\frac{dh}{d\eta}(\eta)$ are given in equations (3) and (5), respectively. Similarly, the total elevator hinge moment transmitted by a section y is

$$h(y) = \int_y^{b_t/2} \frac{dh}{d\eta} d\eta \tag{8}$$

If the boundary condition that the twist is zero at the root is assumed, the angles of twist for the stabilizer and elevator can be expressed in the form

$$\theta(y) = \int_0^y \frac{d\theta}{d\eta} d\eta \tag{9}$$

$$\phi(y) = \int_0^y \frac{d\phi}{d\eta} d\eta \tag{10}$$

The torsional-rigidity coefficients for the stabilizer and elevator, respectively, are defined as

[redacted]

$$C_{TR_s}(\eta) = \frac{t(\eta)}{d\theta/d\eta}$$

$$C_{TR_e}(\eta) = \frac{h(\eta)}{d\phi/d\eta}$$

where $t(\eta)$ and $h(\eta)$ refer to the total torque transmitted by a section η. Substitution for $d\theta/d\eta$ and $d\phi/d\eta$ in equations (9) and (10) results in

$$\theta(y) = \int_0^y \frac{t(\eta)}{C_{TR_s}(\eta)} d\eta \qquad (11)$$

$$\phi(y) = \int_0^y \frac{h(\eta)}{C_{TR_e}(\eta)} d\eta \qquad (12)$$

where $t(\eta)$ and $h(\eta)$, corresponding to $t(y)$ and $h(y)$, are given by equations (7) and (8), respectively.

Equations (2), (7), (8), (11), and (12) express, within the limitations of the theory involved, the equilibrium conditions at each section between the aerodynamic and elastic torques. When the aerodynamic, geometric, and structural parameters expressed in these equations have been determined, the three unknown variables θ, ϕ, and c_{l_t} remain. The simultaneous integral equations resulting from the required equilibrium condition generally involve complicated functions for the three unknown variables. In practical cases, however, it has been found convenient to determine the characteristics of the flexible tail by working with the integral equations through a procedure of successive approximations based on an iteration procedure.

Iteration Method

The first approximation to the tail configuration is taken as the one corresponding to an assumed rigid tail; that is, θ and ϕ are both zero, and the elevator deflection δ and geometric angle of attack of the tail α_t

[redacted]

at each section are equal, respectively, to δ_R and α_{t_R}. Corresponding values of $c_{l_{t_0}}(y)$ are then determined from equation (2). Substitution of these values of $c_{l_{t_0}}(y)$ in equations (3) and (5) gives $\frac{dT}{d\eta}(\eta)$ and $\frac{dh}{d\eta}(\eta)$, and the functions $t_0(y)$, $h_0(y)$, $\theta_1(y)$, and $\phi_1(y)$ can be determined, respectively, from equations (7), (8), (11), and (12). The values thus determined for θ_1 and ϕ_1 can then be employed in turn to determine, successively, new increments in the c_{l_t}, θ, and ϕ distributions. The series resulting from the addition of the successive increments permit the determination of the control characteristics for the flexible tail.

The general procedure for determining the elevator effectiveness of the flexible tail is as follows: Assume, as a first approximation, that the geometric angle of attack $\alpha_t(y)$ is equal to zero and the elevator deflection $\delta(y)$ is equal to δ_R. Compute $c_{l_{t_0}}(y)$ from equation (2). Obtain values for $dT/d\eta$ and $dh/d\eta$ at several spanwise stations from equations (3) and (5), respectively, with $\delta(y) = \delta_R$ and $c_{l_t}(y) = c_{l_{t_0}}(y)$. Integrate equations (7) and (8) to obtain, respectively, $t_0(y)$ and $h_0(y)$. Substitute the values of $t_0(y)$ and $h_0(y)$ corresponding to $t_0(\eta)$ and $h_0(\eta)$ into equations (11) and (12), respectively, and obtain $\theta_1(y)$ and $\phi_1(y)$ as a first approximation to the twist distributions. For the second iteration (first twist iteration), assume that $\delta(y) = \phi_1(y) - \theta_1(y)$ and that $\alpha_t(y) = \theta_1(y)$ and compute the corresponding $c_{l_{t_1}}$ distribution from equation (2). The substitutions and integrations in equations (3), (5), (7), (8), (11), and (12) with $\delta = \phi_1 - \theta_1$ and $c_{l_t} = c_{l_{t_1}}$ in the manner described for the previous iteration then provide the second twist increments $\theta_2(y)$ and $\phi_2(y)$. For the next iteration, assume $\delta(y) = \phi_2(y) - \theta_2(y)$ and $\alpha_t(y) = \theta_2(y)$ and obtain, as described previously, the third twist increments, $\theta_3(y)$ and $\phi_3(y)$. This iteration procedure is continued until the increments for c_{l_t}, θ, and ϕ become negligible.

[redacted]

The foregoing procedure for obtaining the distributions c_{l_t}, θ, and ϕ is summarized in the following table, which gives the variables employed in each iteration:

Variable \ Order of twist iteration	0	1	2	3
θ	0	θ_1	θ_2	θ_3
ϕ	0	ϕ_1	ϕ_2	ϕ_3
α_t	0	θ_1	θ_2	θ_3
δ	δ_R	$(\phi_1 - \theta_1)$	$(\phi_2 - \theta_2)$	$(\phi_3 - \theta_3)$
c_{l_t}	$c_{l_{t_0}}$	$c_{l_{t_1}}$	$c_{l_{t_2}}$	$c_{l_{t_3}}$

In applications of the method of iteration, it will be found that in many cases various approximations may be employed quite advantageously. Thus, for the first and second iterations, the equivalent geometric angle-of-attack distribution can often be approximated by uniform and linear distributions, respectively, so that the c_{l_t} distribution may be obtained directly from the data of reference 7, which gives results for a wide range of taper ratios including the low aspect ratios commonly employed on tails. In other cases, an approximation to the c_{l_t} distribution can be obtained rapidly by the method given in reference 8.

The fact that the method of iteration is based on a procedure in which the twist obtained from each iteration is used to initiate the torque and the twist of the succeeding iteration permits, in many cases, a rapid estimation of the twist distributions for the higher-order iterations. Thus, inasmuch as the twist for a given torque distribution is directly proportional to the magnitude of the torque, it follows that the proportionality of the twists obtained at a section in succeeding iterations will depend on the similarity for the two iterations of the distributions of torque. (See equations (11) and (12).) Because the shapes of the torque and hinge-moment distributions $t(y)$ and $h(y)$ (equations (7) and (8)) for a particular tail are usually not very sensitive to the spanwise variations of θ and ϕ, the shapes of the twist distributions tend to resemble the corresponding twist distributions

[redacted]

that initiated them. In these cases, therefore, the twist distributions for a higher-order iteration may be estimated from a knowledge of the values obtained in the preceding iteration by taking the ratio of the twists for two consecutive iterations at any suitable reference station. The twist θ at any station for the iteration of order n is then given by

$$\theta_n(y) = \left[\frac{(\theta_{n-1})^2}{\theta_{n-2}}\right]_{\text{reference station}}$$

A similar procedure may be followed to estimate the increments in ϕ and c_{l_t} for the higher-order iterations.

The foregoing iteration procedure leads to series of the form

$$c_{l_t} = c_{l_{t_0}} + c_{l_{t_1}} + c_{l_{t_2}} + c_{l_{t_3}} + \ldots$$

$$\theta = \theta_0 + \theta_1 + \theta_2 + \theta_3 + \ldots$$

$$\phi = \phi_0 + \phi_1 + \phi_2 + \phi_3 + \ldots$$

From the formulas derived in the preceding section, the quantities $c_{l_{t_1}}$, θ_1, and ϕ_1 will be noted to contain the dynamic pressure q as a factor; $c_{l_{t_2}}$, θ_2, and ϕ_2, which are dependent on the corresponding values obtained in the preceding iteration, contain q^2; and so on. The lift coefficient and twist at a section may each be represented, therefore, by a power series in q. The coefficients of these series, which depend on the various aerodynamic, geometric, and structural parameters, in general vary with speed because of modifications in the aerodynamic characteristics of the tail introduced principally through the effects of compressibility.

By the application of these iteration procedures, the elevator contribution to the pitching moment about the airplane center of gravity is obtained from equation (1) as follows:

[redacted]

$$M = \left[-l_{tq} \int_{-b_t/2}^{b_t/2} \left(c_{l_{t_0}} + c_{l_{t_1}} + c_{l_{t_2}} + \ldots \right) c_t \, dy + \left(T_0 + T_1 + T_2 \ldots \right) \right] \quad (13)$$

where the numerical subscripts refer to the order of the twist iteration and $T_n = 2\left[t_n(0) + h_n(0)\right]$. (See equations (7) and (8).) Equation (13) may be written

$$M = M_0 + M_1 + M_2 + \ldots \quad (14)$$

The elevator reversal speed is obtained from the value of the dynamic pressure q that makes the right-hand side of equation (14) equal to zero.

In a similar manner, the elevator hinge moment for the flexible tail may be obtained as

$$H = H_0 + H_1 + H_2 + \ldots \quad (15)$$

where $H_n = 2h_n(0)$.

An iteration procedure similar to that described for the elevator effectiveness may be followed to determine the effect of angle of attack of the tail and expressions for M and H similar in form to equations (14) and (15) will be obtained.

The tendency noted previously with regard to the similarity in the respective distributions for θ, ϕ, and c_{l_t} for the higher-order iterations will lead in many cases to considerable simplification in the iteration procedure for determining the effect of tail flexibility on the pitching moment M and the hinge moment H. The increments in M and H for the higher-order iterations can therefore be obtained in these cases by means of the following relationships:

$$M_n = \frac{M_{n-1}^2}{M_{n-2}} \quad (16)$$

$$H_n = \frac{H_{n-1}^2}{H_{n-2}} \quad (17)$$

[redacted]

The forces and resulting twists on the tail structure are directly proportional to the tail angle of attack and the elevator deflection corresponding to the values that would be obtained in an assumed rigid structure or to α_{t_R} and δ_R, respectively. (See table III.) The differentiation of equations (14) and (15) with respect to α_{t_R} and δ_R and conversion to the nondimensional form gives, therefore, for the flexible tail the parameters $\frac{\partial C_m}{\partial \delta_R}$, $\frac{\partial C_m}{\partial \alpha_{t_R}}$, $\frac{\partial C_h}{\partial \delta_R}$, and $\frac{\partial C_h}{\partial \alpha_{t_R}}$.

Corrections for Compressibility

Inasmuch as the aerodynamic charteristics of the tail are affected to an important extent by compressibility, the effects of compressibility must be considered in predictions for the control characteristics of the tail. In the absence of experimental data, the following corrections for compressibility, based on the theory of small perturbations, which is discussed in more detail in reference 9, are summarized for the parameters involved in the present analysis. These corrections may be applied at speeds below that at which the critical compressibility effects occur or up to a Mach number of approximately 0.60 in conventional airplanes.

The span-load distribution in a compressible flow should be computed on the basis of a fictitious aspect ratio equal to the true aspect ratio, reduced by the factor $\sqrt{1 - M^2}$, and the resulting values of c_{l_t} obtained for this reduced fictitious aspect ratio should be multiplied by $1/\sqrt{1 - M^2}$. Thus, if the primes denote values obtained for the fictitious airplane,

$$A_t' = A_t\sqrt{1 - M^2}$$

and

$$c_{l_t} = \frac{c_{l_t}'}{\sqrt{1 - M^2}}$$

[redacted]

The values for the parameters $\left(\frac{\partial c_m}{\partial \delta_R}\right)_{c_{l_t}}$ and $\left(\frac{\partial c_h}{\partial \delta_R}\right)_{c_{l_t}}$ as obtained from low-speed data should be multiplied by the factor $1/\sqrt{1 - M^2}$.

The slope of the lift-coefficient curve in three-dimensional incompressible flow is corrected for compressibility by multiplying it by the factor

$$B = \frac{EA_t + 2}{E'A_t' + 2}$$

in which the symbols E and E' represent the potential-flow correction for chord effect in incompressible and compressible flow, respectively. This correction applies specifically to elliptical plan forms but is approximately correct for other plan forms. In incompressible flow, E is the ratio of the semiperimeter of the ellipse to the span of the airfoil, as indicated in reference 10. In compressible flow, the ratio E' is that for the fictitious elliptical tail of span b_t and aspect ratio A_t'.

The derivative $d\epsilon/d\alpha_w$ for compressible flow is computed on the basis of a fictitious tail length equal to the true tail length increased by the factor $1/\sqrt{1 - M^2}$, and the fictitious aspect ratios for the wing and tail equal to the true aspect ratios reduced by the factor $\sqrt{1 - M^2}$.

APPLICATION OF METHOD

Data for Calculations

Calculations were made by the foregoing procedure of iterations for the effect of tail flexibility on the longitudinal control characteristics for two modern fighter airplanes designated airplanes A and B in order to illustrate the method and to obtain quantitative results for some typical cases. The computations were made, for both airplanes, of the tail effectiveness, the hinge-moment characteristics, and the control-force gradients required in recovery from dives at sea level and at an altitude of 30,000 feet.

[redacted]

Figures 1 and 2 show the plan forms and dimensions of the horizontal tails for airplanes A and B, respectively. These figures also give the location of the flexural axis as determined from stabilizer torsional-rigidity tests made in connection with the present investigation. The torsional-rigidity tests for airplane A were made by the Langley Flight Research Division and for airplane B by the Langley Aircraft Loads Division. Both the stabilizer and the elevator for airplane A are metal covered, whereas airplane B has a metal-covered stabilizer and a fabric-covered elevator.

The aerodynamic parameters for the two airplanes were based on low-speed data corrected for compressibility effects, essentially as described previously. The basic data employed in the calculations, the source from which these data were obtained, and the compressibility corrections applied are given in tables I and II. Average values along the span were assumed for the parameters $\left(\frac{\partial c_h}{\partial \delta_R}\right)_{c_{l_t}}$ and $\left(\frac{\partial c_h}{\partial c_{l_t}}\right)_{\delta_R}$, which were obtained on the basis of estimates for $\partial C_h/\partial \delta_R$ and $\partial C_h/\partial \alpha_{t_R}$ from low-speed flight data. In the computations, the aerodynamic centers of the tail sections were assumed to be at the quarter-chord points of the sections.

The tail-stiffness data for the calculations were obtained from flexibility tests made on the stabilizer and elevator of the full-size airplanes. In order to clarify the relationship of the flexibility-test results to actual flight conditions, the procedure for the determination of the stiffness data is described herein in some detail. The stabilizer tests were made by applying a concentrated torsional couple at a section near one tip of the stabilizer and measuring the torsional deflections at several stations along the span with reference to a station on the unloaded half of the stabilizer. The elevator-flexibility tests were made by loading bags containing lead shot or sand on one-half of the elevator along a line one-third of the chord behind the hinge with the elevator locked in position. The spanwise loading on the elevator surface corresponded approximately to a uniform distribution. The deflections of the elevator on the loaded side were measured at

[redacted]

several stations with respect to a reference station taken on the unloaded half of the elevator.

Tests were also performed on one rib of the elevator of airplane B at a station about 4.5 feet from the fuselage center line to obtain the effect on the distortion along the chord of a chordwise loading that simulated a triangular distribution more closely than the one just described (load concentrated at one-third of chord behind hinge). In these tests, measurements were taken of the deflections at very small intervals along the chord (5 dial gages for an 11-inch chord). The results indicated that with both types of loading the distortions along the chord were equal and that the deflections along the chord followed a straight line. It was assumed, therefore, that the measured angular deflection due to the elevator flexibility could be considered as an equivalent change in elevator deflection with no change in the camber of the elevator surface.

The tail-stiffness data for airplane A are shown in figure 3. The results for the stabilizer given in this figure are based on a concentrated torque of 833 foot-pounds applied to the right half of the stabilizer at a station 6.50 feet from the fuselage center line, and the data for the elevator are based on a total hinge moment of 83.3 foot-pounds distributed on the right half of the elevator in the manner described previously.

The tail-stiffness data for airplane B are shown in figure 4. The results for the stabilizer given in this figure are based on a concentrated torque of 500 foot-pounds applied to the left half of the stabilizer at a station 5.92 feet from the fuselage center line, and the elevator data in figure 4 are based on a total hinge moment of 60 foot-pounds distributed on the right half of the elevator in the manner described previously.

Procedure for Calculations

With the aid of the foregoing data, the spanwise distributions for cl_t, θ, and ϕ were determined for several iterations. The cl_t distributions were obtained by the usual methods based on lifting-line theory. In the computations, the stabilizers for the two airplanes were assumed to act in torsion similarly to tubes so that

[redacted]

the distributions of stabilizer twist resulting from the aerodynamic forces were calculated by means of equations (7) and (11) by use of the stabilizer torsional-rigidity coefficients shown in figures 3 and 4. Because the results of the elevator-flexibility tests for both airplanes indicated the probability that the static loads on the elevator did not act in pure torsion (see figs. 3 and 4 for $d\phi/dH$ near root and tip sections), it was believed practical in the present investigation to modify the method described previously for determining ϕ. The twist distributions due to elevator flexibility were obtained, therefore, by multiplying the total hinge moment acting on each half of the elevator by the rigidity factors $\frac{d\phi}{dH}(y)$ shown in figures 3 and 4. This method for determining the elevator twist is strictly correct only if the loading on the elevator surface in the static tests simulated the loading in flight. For the present investigation, however, the error from this source is not expected to be important. Some computations with different assumed elevator flexibilities, which are discussed in the section entitled "Results and Discussion", indicate that the calculated results are not sensitive to reasonable variations in the elevator flexibility.

The increments for c_{l_t}, θ, and ϕ that were obtained in the various iterations were used to compute the pitching moment about the airplane center of gravity M by means of equations (13) and (14) and to compute the elevator hinge moment H by means of the corresponding equation (15). The results for M and H were then converted into the nondimensional form as the derivatives $\partial C_m/\partial \alpha_{t_R}$, $\partial C_m/\partial \delta_R$, $\partial C_h/\partial \alpha_{t_R}$, and $\partial C_h/\partial \delta_R$. The details of the computations for determining $\partial C_m/\partial \delta_R$ and $\partial C_h/\partial \delta_R$ for airplane B for a Mach number of 0.60 at sea level are shown in table III.

The change in control force per unit change in normal acceleration in recovery from a dive was computed by means of the following formula:

$$F_n = \left(\frac{\partial C_h}{\partial \delta_R}\Delta\delta_R + \frac{\partial C_h}{\partial \alpha_{t_R}}\Delta\alpha_{t_R}\right) K_e q \bar{c}_e^2 b_e \qquad (18)$$

[redacted]

where $\Delta\delta_R$ and $\Delta\alpha_{t_R}$ refer to the changes in δ_R and α_{t_R} per unit change in normal acceleration in terms of g and where K_e is the elevator gearing ratio. In equation (18)

$$\Delta\delta_R = \frac{1}{q}\left\{\frac{W}{S\frac{\partial C_m}{\partial \delta_R}}\left[\frac{\partial C_{m_R}}{\partial \delta_R}\left(\frac{d\delta_R}{dC_L}\right)_R - \frac{1-\frac{d\epsilon}{d\alpha_w}}{a}\left(\frac{\partial C_m}{\partial \alpha_{t_R}} - \frac{\partial C_{m_R}}{\partial \alpha_{t_R}}\right)\right]\right.$$

$$\left. + 28.6 l_t \rho g \left(\frac{d\delta_R}{d\alpha_{t_R}}\right)_{C_m}\right\} \qquad (19)$$

and

$$\Delta\alpha_{t_R} = \frac{1}{q}\left[\frac{W}{Sa}\left(1 - \frac{d\epsilon}{d\alpha_w}\right) + 28.6 l_t \rho g\right] \qquad (20)$$

In equation (19) the two terms on the right-hand side enclosed in the brackets represent the part of $\Delta\delta_R$ required to trim the airplane, and the third term represents the part of $\Delta\delta_R$ required to balance the effects of rotation of the tail during the steady phase of the pitching motion. In these equations, $\partial C_h/\partial \delta_R$, $\partial C_h/\partial \alpha_{t_R}$, $\partial C_m/\partial \delta_R$, $\partial C_m/\partial \alpha_{t_R}$, and $\left(\frac{\partial \delta_R}{\partial \alpha_{t_R}}\right)_{C_m}$ are the values for the flexible tail obtained by the iteration procedure. If values for these parameters for the assumed rigid tail are used in equations (18), (19), and (20), the control-force gradient for the rigid tail F_{n_R} is obtained. The values for the derivative $\left(\frac{d\delta_R}{dC_L}\right)_R$ for airplanes A and B were based on flight results at an indicated airspeed of approximately 200 miles per hour. A value of $\left(\frac{d\delta_R}{dC_L}\right)_R$ equal

[redacted]

to -3.20 was obtained for airplane A based on a center-of-gravity location of 28 percent of the mean aerodynamic chord; whereas a value of -3.26 was obtained for airplane B based on a center-of-gravity location of 29.5 percent of the mean aerodynamic chord. The effect on F_n and F_{n_R} of movements of the airplane center of gravity was investigated by assuming different values for $\left(\frac{d\delta_R}{dC_L}\right)_R$.

The variation of $\frac{d\epsilon}{d\alpha_w}$ with speed as determined by means of the theoretical compressibility corrections noted previously, in conjunction with the design charts of reference 11, indicated a negligible change in this parameter up to a Mach number of 0.60. It was therefore considered sufficiently accurate in the present computations to assume constant values for $d\epsilon/d\alpha_w$. The values for $\left(\frac{d\delta_R}{dC_L}\right)_R$, however, were corrected for compressibility effects by multiplying the low-speed value by the factor $1/B$ corresponding to an average between the wing and tail.

RESULTS AND DISCUSSION

The results of the calculations are presented in table III and in figures 5 to 9. Table III shows the results obtained for the various iterations in determining $\partial C_m/\partial\delta_R$ and $\partial C_h/\partial\delta_R$ for airplane B at a Mach number of 0.60 at sea level. Figure 5 shows the spanwise variation of tail angle of attack α_t and elevator deflection δ resulting from an application of the elevator control equivalent to unit deflection for the assumed rigid tail, as obtained from table III. Figures 6 to 9 show the effects of horizontal-tail flexibility on the longitudinal control characteristics for airplanes A and B for a range of true airspeeds from 0 to 550 miles per hour at sea level and from 0 to 490 miles per hour at an altitude of 30,000 feet. This range of true airspeed corresponds to a Mach number range from 0 to 0.72. The speed for each altitude corresponding to a Mach number of 0.60, which represents

[redacted]

the limit for which the theoretical compressibility corrections employed in the present computations are believed to be reliable, is indicated on figures 6 to 9. The results for the Mach numbers higher than 0.60 are included in the figures in order to give an indication of the trend of the flexibility effects. The results of the computations for a Mach number of 0.60 at sea level are summarized for both airplanes in table IV.

Table III indicates that the convergence of the iteration prccedure is very rapid. This convergence, as indicated for $\partial C_m/\partial \delta_R$ and $\partial C_h/\partial \delta_R$ for airplane B, is typical for the other parameters in the flexible tail for both airplanes. Thus, if the contribution obtained for each successive iteration is expressed as a ratio of that obtained for the zeroth-order twist iteration,

$$\left.\begin{aligned} \frac{\partial C_m/\partial \delta_R}{\partial C_{m_R}/\partial \delta_R} &= 1 - 0.301 + 0.0727 - 0.0167 + 0.00384 = 0.759 \\ \frac{\partial C_h/\partial \delta_R}{\partial C_{h_R}/\partial \delta_R} &= 1 - 0.241 + 0.0557 - 0.0131 + 0.00306 = 0.805 \end{aligned}\right\} \quad (21)$$

The subsequent comparison illustrates the number of twist iterations required by the regular procedure of iteration in order to determine the longitudinal control characteristics for a flexible tail. The results obtained from table III as given by equations (21), which utilized three regular twist iterations, will be compared with results obtained by the use of one and two regular twist iterations, respectively, in conjunction with the relationships given by equations (16) and (17) for estimating M_n and H_n for the twist iterations of higher order than one and two, respectively. Thus, by use of one regular twist iteration,

$$\left.\begin{aligned} \frac{\partial C_m/\partial \delta_R}{\partial C_{m_R}/\partial \delta_R} &= 1 - 0.301 + 0.0905 - 0.0272 + 0.00815 = 0.771 \\ \frac{\partial C_h/\partial \delta_R}{\partial C_{h_R}/\partial \delta_R} &= 1 - 0.241 + 0.0581 - 0.0140 + 0.00338 = 0.806 \end{aligned}\right\} \quad (22)$$

[redacted]

By use of two regular twist iterations,

$$\left.\begin{aligned}\frac{\partial C_m/\partial \delta_R}{\partial C_{m_R}/\partial \delta_R} &= 1 - 0.301 + 0.0727 - 0.0176 + 0.00425 = 0.759 \\ \frac{\partial C_h/\partial \delta_R}{\partial C_{h_R}/\partial \delta_R} &= 1 - 0.241 + 0.0557 - 0.0129 + 0.00300 = 0.805\end{aligned}\right\} \quad (23)$$

The comparison of the results shown in equations (22) with those given by equations (21) indicates that the use of one regular twist iteration in conjunction with the simple relationships given by equations (16) and (17) is sufficient to determine the effect of tail flexibility to an accuracy of the order of 1 percent.

Figures 6 and 7 show for airplanes A and B, respectively, the ratio of the tail effectiveness and hinge-moment parameters as obtained in the actual flexible tail to those obtained for the assumed rigid tail. These figures indicate, for the complete range of airspeeds for both airplanes, that the parameters $\partial C_m/\partial \delta_R$, $\partial C_m/\partial \alpha_{t_R}$, $\partial C_h/\partial \delta_R$, and $\partial C_h/\partial \alpha_{t_R}$ are reduced numerically because of the tail flexibility and that the parameters $\left(\frac{\partial \delta_R}{\partial \alpha_{t_R}}\right)_{C_m}$ and $\frac{\partial C_h/\partial \delta_R}{\partial C_m/\partial \delta_R}$ are increased numerically because of this factor. The numerical reduction in $\partial C_m/\partial \delta_R$ caused by tail flexibility is due to the fact that the center of pressure of the lift resulting from the elevator deflection is behind the flexural axis (see figs. 1 and 2 for flexural-axis locations) and the resulting torsional moment twists the stabilizer in a manner that reduces the tail lift. The numerical reduction in $\partial C_m/\partial \delta_R$ is also due to the negative value of $\partial C_h/\partial \delta_R$, which causes the elevator to twist and thus to reduce the elevator deflection.

[redacted]

The numerical reduction in $\partial C_m/\partial \alpha_{t_R}$ due to tail flexibility resulted because the location of the flexural axis of the stabilizer is ahead of the aerodynamic center and because the value of $\partial C_h/\partial \alpha_{t_R}$ is negative. The respective numerical reduction in the values for $\partial C_h/\partial \delta_R$ and $\partial C_h/\partial \alpha_{t_R}$ due to the tail flexibility resulted principally from the fact that each of these parameters for the rigid tail is negative and the elevator twist therefore numerically reduces the hinge moment in each case. The forward position of the stabilizer flexural axis relative to the center of pressure of the lift contributed by the elevator tended, however, to increase numerically the value of $\partial C_h/\partial \delta_R$ due to the stabilizer twist (δ is increased by $-\theta$); similarly, the location of the flexural axis of the stabilizer ahead of its aerodynamic center tended to increase numerically the value for $\partial C_h/\partial \alpha_{t_R}$.

Figures 6 and 7 indicate that, in general, the effects of tail flexibility vary with speed and altitude approximately as the dynamic pressure - modified, of course, by the relative compressibility effects. This variation with speed and altitude results from the rapid convergence of the power series in q, which causes the terms in q of higher order than unity to be comparatively small. In some cases, however, at very high speeds (see figs. 7(b) and 8, for $\frac{\partial C_h/\partial \alpha_{t_R}}{\partial C_{h_R}/\partial \alpha_{t_R}}$ and F_n/F_{n_R}, respectively), the effects of the terms in q of higher power than unity become comparatively significant.

Computations were made to estimate the effect on the parameters shown in figures 6 and 7 of increasing the elevator stiffness at each section by 12.5 percent of the average elevator stiffness. The results of these computations indicated that, for a Mach number of 0.60 at sea level, the ratios of the parameters $\partial C_m/\partial \delta_R$, $\partial C_h/\partial \delta_R$, and $\partial C_h/\partial \alpha_{t_R}$ to the corresponding ratios for the assumed rigid tail would be increased in the order of 2.5 percent as compared with those shown in figures 6 and 7, and the corresponding ratio for $\partial C_m/\partial \alpha_{t_R}$ would be increased by less than 1 percent; whereas, at 30,000 feet for the same Mach number, the effect of the

[redacted]

increased elevator stiffness would be about 0.40 of the corresponding foregoing effects indicated at sea level.

It can be noted from figures 6 and 7 that, provided critical compressibility effects do not appear, elevator reversal for both airplanes A and B does not occur up to a speed corresponding to a Mach number of 0.72.

Figures 8 and 9 present a comparison of the control-force gradients in recovery from dives as obtained for the actual flexible tail and assumed rigid tail. It should be noted in these figures that the required motions of the elevator control stick per unit g are not necessarily equal for the flexible and assumed rigid tails. Figure 8 gives the results for airplane A at sea level and at an altitude of 30,000 feet. This figure shows the variation with airspeed of F_n and the ratio F_n/F_{n_R} for values of $\left(\frac{d\delta_R}{dC_L}\right)_R$ in incompressible flow of -3.2 and -1.60. These values of -3.2 and -1.60 correspond, respectively, to center-of-gravity locations at 28 percent and approximately 31 percent of the mean aerodynamic chord. Figure 8 shows that flexibility of the tail increases the control-force gradient and that this increase for a Mach number of 0.60 amounts to 12 percent at sea level and 3.5 percent at 30,000 feet altitude. This figure also shows that a rearward movement of the center of gravity of approximately 3 percent of the mean aerodynamic chord causes a small reduction in the ratio F_n/F_{n_R}. The results for the airplane B at sea level and at altitude for values of $\left(\frac{d\delta_R}{dC_L}\right)_R$ in incompressible flow of -3.26 and -6.00 are presented in figure 9. These values of -3.26 and -6.00 correspond, respectively, to center-of-gravity locations at 29.5 percent and approximately 25 percent of the mean aerodynamic chord. The figure shows, for airplane B for a range of airspeeds at the altitudes considered, a small increase in the control-force gradient due to tail flexibility, or approximately one-half of that indicated in figure 8 for airplane A. Figure 9 also shows that a forward movement of the center of gravity of approximately 4.5 percent of the mean aerodynamic chord causes a small increase in the ratio F_n/F_{n_R}.

[redacted]

An examination of equations (18), (19), and (20) indicates that the control-force gradient in a dive recovery may be influenced to an important extent by the aerodynamic parameters $\frac{\partial C_h/\partial \delta_R}{\partial C_m/\partial \delta_R}$, $\partial C_h/\partial \alpha_{t_R}$, and $\partial C_m/\partial \alpha_{t_R}$. The results of the present analysis show for both airplanes A and B that the first two of these parameters are affected by tail flexibility in a manner to increase F_n; whereas $\partial C_m/\partial \alpha_{t_R}$ is affected by this factor in a manner to reduce F_n. As noted previously, the numerical reduction in $\partial C_m/\partial \alpha_{t_R}$ obtained in the present computations for airplanes A and B is caused principally by the location of the flexural axis of the stabilizer ahead of its aerodynamic center and by the negative value of $\partial C_h/\partial \alpha_{t_R}$. In order to obtain an indication of the importance of the change in $\partial C_m/\partial \alpha_{t_R}$ due to tail flexibility for the control-force gradient in a dive recovery, computations were made for the two airplanes in which it was assumed that $\frac{\partial C_m}{\partial \alpha_{t_R}} = \frac{\partial C_{m_R}}{\partial \alpha_{t_R}}$, which is roughly equivalent in the present case to a rearward movement of the flexural axis back to the aerodynamic center. These computations indicated, for a Mach number of 0.60 at sea level, that in the case of airplane A the ratio F_n/F_{n_R} would be increased from 1.12 to 1.26, and in the case of airplane B this ratio would be increased from 1.03 to 1.075. On the basis of the present analysis it appears, therefore, that the location of the flexural axis of the stabilizer too far behind the aerodynamic center of the tail, could cause excessive control forces in a dive recovery at high speeds.

CONCLUSIONS

An iteration method for determining the effect of tail flexibility on the longitudinal control characteristics of airplanes was applied to two modern fighter airplanes and was found to provide a practical procedure for the determination of these effects.

[redacted]

The results of calculations to determine the effect of tail flexibility on the longitudinal control characteristics for two fighter airplanes indicate that the longitudinal control characteristics are affected to a significant extent at high speeds by this factor. The following conclusions apply to results for these airplanes at speeds below that at which critical compressibility effects occur:

1. The magnitude of the tail-flexibility effects, in general, varied approximately as the dynamic pressure - modified, of course, by the relative compressibility effects. In some cases at very high speeds, however, the effects of the terms containing the dynamic pressure of powers greater than unity became comparatively significant.

2. Tail flexibility was found to reduce significantly the rates of change of pitching moment and hinge moment with elevator deflection and tail angle of attack.

3. The control-force gradients in a dive recovery were increased because of tail flexibility.

4. Rearward movements of the airplane center of gravity tended to decrease the effects of the tail flexibility on the control-force gradient; whereas forward movements of the airplane center of gravity tended to increase the magnitude of these effects.

5. The location of the flexural axis of the stabilizer relative to the aerodynamic center of the tail is an important design consideration with regard to the magnitude of the tail-flexibility effects. The location of the flexural axis of the stabilizer too far behind the aerodynamic center could cause excessive control forces in a dive recovery at high speeds.

Langley Memorial Aeronautical Laboratory
National Advisory Committee for Aeronautics
Langley Field, Va.

[redacted]

REFERENCES

1. Collar, A. R., and Grinstead, F.: The Effect of Structural Flexibility of Tailplane, Elevator, and Fuselage of Longitudinal Control and Stability. Rep. No. S. M. E. 3227, British R.A.E., Sept. 1942, and Addendum, Rep. No. S. M. E. 3227a. Oct. 1942.

2. Glauert, H.: The Elements of Aerofoil and Airscrew Theory. Cambridge Univ. Press, 1926.

3. Pearson, H. A.: Span Load Distribution for Tapered Wings with Partial-Span Flaps. NACA Rep. No. 585, 1937.

4. Hildebrand, Francis B.: A Least-Squares Procedure for the Solution of the Lifting-Line Integral Equation. NACA TN No. 925, 1944.

5. Trayer, George W., and March H. W.: The Torsion of Members Having Sections Common in Aircraft Construction. NACA Rep. No. 334, 1930.

6. Timoshenko, S.: Theory of Elasticity. First ed. McGraw-Hill Book Co., Inc., 1934.

7. Anderson, Raymond F.: Determination of the Characteristics of Tapered Wings. NACA Rep. No. 572, 1936.

8. Schrenk, O.: A Simple Approximation Method for Obtaining the Spanwise Lift Distribution. NACA TM No. 948, 1940.

9. Goldstein, S., and Young, A. D.: The Linear Perturbation Theory of Compressible Flow, with Applications to Wind-Tunnel Interference. 6865, Ae. 2262, F.M. 601, British A.R.C., July 6, 1943.

10. Jones, Robert T.: Correction of the Lifting-Line Theory for the Effect of the Chord. NACA TN No. 817, 1941.

11. Silverstein, Abe, and Katzoff, S.: Design Charts for Predicting Downwash Angles and Wake Characteristics behind Plain and Flapped Wings. NACA Rep. No. 648, 1939.

[redacted]

12. Ames, Milton B., Jr., and Sears, Richard I.: Determination of Control-Surface Characteristics from NACA Plain-Flap and Tab Data. NACA Rep. No. 721, 1941.

[redacted]

TABLE I

DATA FOR CALCULATIONS - PHYSICAL AND GEOMETRIC CHARACTERISTICS

[Data furnished by manufacturer]

Airplane	Weight, W (lb)	Wing area, S (sq ft)	Wing aspect ratio	Mean aerodynamic chord of wing, c_w (ft)	Tail area, S_t (sq ft)	Elevator span, b_e (sq ft)	Root mean chord of elevator, $\bar{c}_e$ (ft)	Tail length, l_t (ft)	K_e (radian/ft)
A	12,000	300	5.55	7.28	55	16	1.19	21.4	0.66
B	7,660	236	5.815	6.64	41.1	13.2	1.01	15.5	.57

TABLE II

DATA FOR CALCULATIONS - AERODYNAMIC PARAMETERS

Parameter	Value in incompressible flow	Source of data	Correction for compressibility
Airplane A			
$(\partial c_m/\partial \delta_R)_{c_{l_t}}$	[a]-0.0086	Reference 12	Multiply by $\frac{1}{\sqrt{1-M^2}}$
a_o	0.095	Assumed	Do.
$(\partial c_h/\partial \delta_R)_{c_{l_t}}$	-0.00686	Unpublished data based on $\partial C_h/\partial \alpha_{t_R}$ = -0.00218 and $\partial C_h/\partial \delta_R$ = -0.00804	Do.
$(\partial c_h/\partial c_{l_t})_{\delta_R}$	-0.0352		None
$(\partial \alpha_{t_R}/\partial \delta_R)$	[a]-0.66	Reference 12	None
$d\epsilon/d\alpha_w$	0.50	Reference 11	Assumed constant
	0.077	Reference 7	Multiply by B
$(\partial \delta_R/dC_L)_R$	-3.2	Based on unpublished data for c.g. at 28 percent M.A.C.	Multiply by 1/B; average for wing and tail
Airplane B			
$(\partial c_m/\partial \delta_R)_{c_{l_t}}$	[b]-0.0091	Reference 12	Multiply by $\frac{1}{\sqrt{1-M^2}}$
a_o	0.095	Assumed	Do.
$(\partial c_h/\partial \delta_R)_{c_{l_t}}$	-0.00605	Estimated from unpublished flight data based on $\partial C_h/\partial \alpha_{t_R}$ = -0.000511 and $\partial C_h/\partial \delta_R$ = -0.00635	Do.
$(\partial c_h/\partial c_{l_t})_{\delta_R}$	-0.00825		None
$(\partial \alpha_{t_R}/\partial \delta_R)_{c_{l_t}}$	[b]-0.59	Reference 12	None
$d\epsilon/d\alpha_w$	0.50	Reference 11	Assumed constant
a	0.077	Reference 7	Multiply by B
$(\partial \delta_R/dC_L)_R$	-3.26	Estimated from unpublished flight data for c.g. at 29.5 percent M.A.C.	Multiply by 1/B; average for wing and tail

[a]Value given is for a section at 4.5 ft. from fuselage center line; appropriate values were used for other sections.

[b]Average constant values were used.

[redacted]

NATIONAL ADVISORY
COMMITTEE FOR AERONAUTICS

TABLE III.- COMPUTATIONS FOR $\frac{\partial C_m}{\partial \delta_R}$ AND $\frac{\partial C_h}{\partial \delta_R}$ OF AIRPLANE B AT A MACH NUMBER OF 0.60 AT SEA LEVEL

[Compressibility effects have been accounted for in all aerodynamic parameters;

$q = 534.6$; $\left(\frac{\partial C_m}{\partial \delta_R}\right)_{c_{l_t}} = -0.0114$; $\left(\frac{\partial C_h}{\partial \delta_R}\right)_{c_{l_t}} = -0.00756$; $\left(\frac{\partial c_h}{\partial c_{l_t}}\right)_{\delta_R} = -0.00825$]

[redacted]

Distance from center line (ft)	δ	a_t (deg)	c_{l_t} (based on eq. (2))	$\frac{e}{c_t}$ (fig. 2)	c_t^2 (fig. 2)	$\frac{dT}{d\eta}$ (eq.(3))	c_e^2 (fig. 2)	$\frac{dh}{d\eta}$ (eq.(5))	t (eq.(7))	C_{TR_s} (fig. 4)	θ (eq.(11))	$h(0)$ (eq.(8))	$\frac{d\phi}{dH}$ (fig.4)	$\phi = h(0)\frac{d\phi}{dH}$	c_t (fig. 2)
	Zeroth order of twist iteration														
	δ	a_t	$\frac{c_{l_{t_0}}}{\delta_R}$	$\frac{e}{c_t}$	c_t^2	$\frac{dT_0/d\eta}{\delta_R}$	c_e^2	$\frac{dh_0/d\eta}{\delta_R}$	$\frac{t_0}{\delta_R}$	C_{TR_s}	$\frac{\theta_1}{\delta_R}$	$\frac{h_0(0)}{\delta_R}$	$\frac{d\phi}{dH}$	$\frac{\phi_1}{\delta_R}$	c_t
0.375	δ_R	0	0.0425	0.026	16.6	-91.36	1.89	-7.993	-395.2	∞	0	-29.51	0.00634	-0.1871	4.08
1.25	↓	↓	.0440	.008	14.5	-85.65	1.64	-6.945	-324.3	21200	-.00791		.00700	-.2066	3.81
2.50			.0455	-.010	12.0	-78.06	1.37	-5.812	-231.2	10200	-.03229		.00835	-.2464	3.47
3.75			.0450	-.036	9.73	-67.74	1.00	-4.241	-147.6	5560	-.06362		.01110	-.3276	3.12
5.00			.0409	-.068	7.56	-57.31	.765	-3.251	-74.17	2960	-.09645		.01519	-.4483	2.75
5.83			.0342	-.116	6.35	-52.17	.62	-2.598	-31.01	1800	-.11536		.01450	-.4279	2.52
6.60			0	-----	0	------	0	------	0	-----	-.12329		-------	-------	0
	First order of twist iteration														
	$\frac{\phi_1 - \theta_1}{\delta_R}$	$\frac{\theta_1}{\delta_R}$	$\frac{c_{l_{t_1}}}{\delta_R}$	$\frac{e}{c_t}$	c_t^2	$\frac{dT_1/d\eta}{\delta_R}$	c_e^2	$\frac{dh_1/d\eta}{\delta_R}$	$\frac{t_1}{\delta_R}$	C_{TR_s}	$\frac{\theta_2}{\delta_R}$	$\frac{h_1(0)}{\delta_R}$	$\frac{d\phi}{dH}$	$\frac{\phi_2}{\delta_R}$	c_t
0.375	-0.1871	-0.1871	-0.00996	0.026	16.6	16.66	1.89	1.515	100.72	∞	0	7.116	0.00634	0.0452	4.08
1.25	-.1987	-.2066	-.01074	.008	14.5	16.92	1.64	1.400	86.88	21200	.00137		.00700	.0497	3.81
2.50	-.2111	-.2464	-.01277	-.010	12.0	16.46	1.37	1.258	67.16	10200	.00886		.00835	.0595	3.47
3.75	-.2640	-.3276	-.01526	-.036	9.73	18.52	1.00	1.143	46.76	5560	.01841		.01110	.0789	3.12
5.00	-.3519	-.4483	-.01599	-.068	7.56	20.58	.765	1.143	23.21	2960	.02907		.01519	.1080	2.75
5.83	-.3126	-.4279	-.01347	-.116	6.35	17.38	.62	.829	7.89	1800	.03435		.01450	.1032	2.52
6.60	------	------	-------	-----	0	-----	0	-----	------	-----	.03604		-------	-------	0
	Second order of twist iteration														
	$\frac{\phi_2 - \theta_2}{\delta_R}$	$\frac{\theta_2}{\delta_R}$	$\frac{c_{l_{t_2}}}{\delta_R}$	$\frac{e}{c_t}$	c_t^2	$\frac{dT_2/d\eta}{\delta_R}$	c_e^2	$\frac{dh_2/d\eta}{\delta_R}$	$\frac{t_2}{\delta_R}$	C_{TR_s}	$\frac{\theta_3}{\delta_R}$	$\frac{h_2(0)}{\delta_R}$	$\frac{d\phi}{dH}$	$\frac{\phi_3}{\delta_R}$	c_t
0.375	0.04516	0.04520	0.002443	0.026	16.6	-4.007	1.89	-0.3652	-23.16	∞	0	-1.643	0.00634	-0.01042	4.08
1.25	.04776	.04971	.002614	.008	14.5	-4.055	1.64	-.3352	-19.88	21200	-.00041		.00700	-.01150	3.81
2.50	.05059	.05595	.003106	-.010	12.0	-3.901	1.37	-.2983	-15.30	10200	-.00161		.00835	-.01372	3.47
3.75	.05762	.07893	.003719	-.036	9.73	-4.114	1.00	-.2497	-10.60	5560	-.00406		.01110	-.01824	3.12
5.00	.07897	.10801	.003914	-.068	7.56	-4.714	.765	-.2593	-5.32	2960	-.00622		.01519	-.02496	2.75
5.83	.06682	.10321	.003285	-.116	6.35	-3.959	.62	-.1813	-1.86	1800	-.00775		.01450	-.02382	2.52
6.60	-------	------	0	-----	0	------	0	-------	0	-----	-.00821		-------	--------	0

From table I,
$l_t = 15.5$ ft, $S = 236$ sq ft, $c_w = 6.64$ ft
$\bar{c}_e = 1.01$ ft, $b_e = 13.2$ ft

$$\frac{M_0}{\delta_R} = \frac{-2l_t q}{\delta_R}\left(\int_0^{\frac{b_t}{2}} c_{l_{t_0}} c_t d\eta\right) + \frac{2}{\delta_R}\left[t_0(0) + h_0(0)\right]$$

$= -15{,}660$ ft-lb

$$\frac{H_0}{\delta_R} = \frac{2h_0(0)}{\delta_R} = -59.03 \text{ ft-lb}$$

$$\frac{M_1}{\delta_R} = \frac{-2l_t q}{\delta_R}\left(\int_0^{\frac{b_t}{2}} c_{l_{t_1}} c_t d\eta\right) + \frac{2}{\delta_R}\left[t_1(0) + h_1(0)\right]$$

$= 4711$ ft-lb

$$\frac{H_1}{\delta_R} = \frac{2h_1(0)}{\delta_R} = 14.23 \text{ ft-lb}$$

$$\frac{M_2}{\delta_R} = \frac{-2l_t q}{\delta_R}\left(\int_0^{\frac{b_t}{2}} c_{l_{t_2}} c_t d\eta\right) + \frac{2}{\delta_R}\left[t_2(0) + h_2(0)\right]$$

$= -1139$ ft-lb

$$\frac{H_2}{\delta_R} = \frac{2h_2(0)}{\delta_R} = -3.29 \text{ ft-lb}$$

[redacted]

TABLE III.- COMPUTATIONS FOR $\frac{\partial C_m}{\partial \delta_R}$ AND $\frac{\partial C_h}{\partial \delta_R}$ OF AIRPLANE B AT A MACH NUMBER OF 0.60 AT SEA LEVEL - Concluded

Third order of twist iteration

By procedures similar to those given previously $\begin{cases} \frac{M_3}{\delta_R} = 261.6 \text{ ft-lb} \\ \frac{H_3}{\delta_R} = 0.771 \text{ ft-lb} \end{cases}$

Fourth order of twist iteration

By means of equation (16)

$$\frac{M_4}{\delta_R} = -60.08 \text{ ft-lb}$$

By means of equation (17)

$$\frac{H_4}{\delta_R} = -0.1807 \text{ ft-lb}$$

If equations 14 and 15 are employed and the results expressed nondimensionally

$$\frac{\partial C_m}{\partial \delta_R} = \frac{\left(M_0 + M_1 + M_2 + M_3 + M_4\right)/\delta_R}{qSc_w} = -0.0142; \qquad \frac{\frac{\partial C_m}{\partial \delta_R} qSc_w}{M_0} = \frac{\partial C_m/\partial \delta_R}{\partial C_{m_R}/\partial \delta_R} = 0.759$$

$$\frac{\partial C_h}{\partial \delta_R} = \frac{\left(H_0 + H_1 + H_2 + H_3 + H_4\right)/\delta_R}{q\bar{c}_e^2 b_e} = -0.00660; \qquad \frac{\frac{\partial C_h}{\partial \delta_R} q\bar{c}_e^2 b_e}{H_0} = \frac{\partial C_h/\partial \delta_R}{\partial C_{h_R}/\partial \delta_R} = 0.805$$

TABLE IV.- COMPARISON OF EFFECT OF HORIZONTAL-TAIL FLEXIBILITY ON LONGITUDINAL CONTROL CHARACTERISTICS FOR AIRPLANES A AND B AT A MACH NUMBER OF 0.60 AT SEA LEVEL

Parameter ratio	Airplane A	Airplane B
$\frac{\partial C_m/\partial \delta_R}{\partial C_{m_R}/\partial \delta_R}$	0.79	0.76
$\frac{\partial C_m/\partial \alpha_{t_R}}{\partial C_{m_R}/\partial \alpha_{t_R}}$	.97	.98
$\frac{\left(\partial \delta_R/\partial \alpha_{t_R}\right)_{C_m}}{\left(\partial \delta_R/\partial \alpha_{t_R}\right)_{C_{m_R}}}$	1.22	1.30
$\frac{\partial C_h/\partial \delta_R}{\partial C_{h_R}/\partial \delta_R}$	.91	.80
$\frac{\partial C_h/\partial \alpha_{t_R}}{\partial C_{h_R}/\partial \alpha_{t_R}}$	.94	.96
$\frac{\frac{\partial C_h/\partial \delta_R}{\partial C_m/\partial \delta_R}}{\frac{\partial C_{h_R}/\partial \delta_R}{\partial C_{m_R}/\partial \delta_R}}$	1.15	1.06
$\frac{F_n}{F_{n_R}}$	1.12	1.06

NATIONAL ADVISORY
COMMITTEE FOR AERONAUTICS

[redacted]

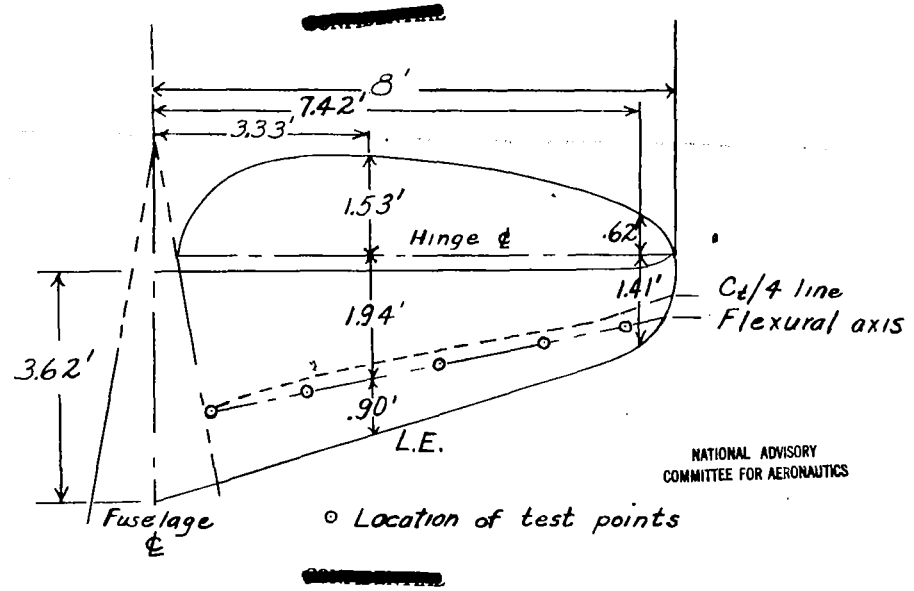

Figure 1.-Plan form of tail semispan showing stabilizer and elevator dimensions. Airplane A; horizontal tail area, 55 square feet; elevator area, 22 square feet; balance area, 17.3 percent of elevator area.

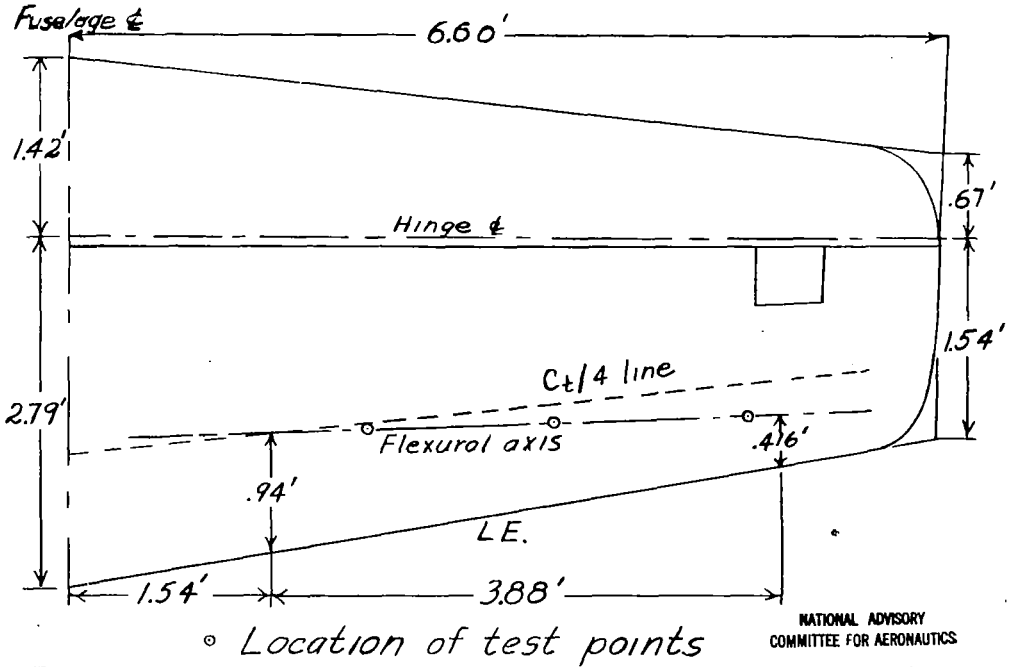

Figure 2.-Plan form of tail semispan showing stabilizer and elevator dimensions. Airplane B; horizontal tail area, 41.1 square feet; elevator area, 13.05 square feet; balance area, 0.24 square feet.

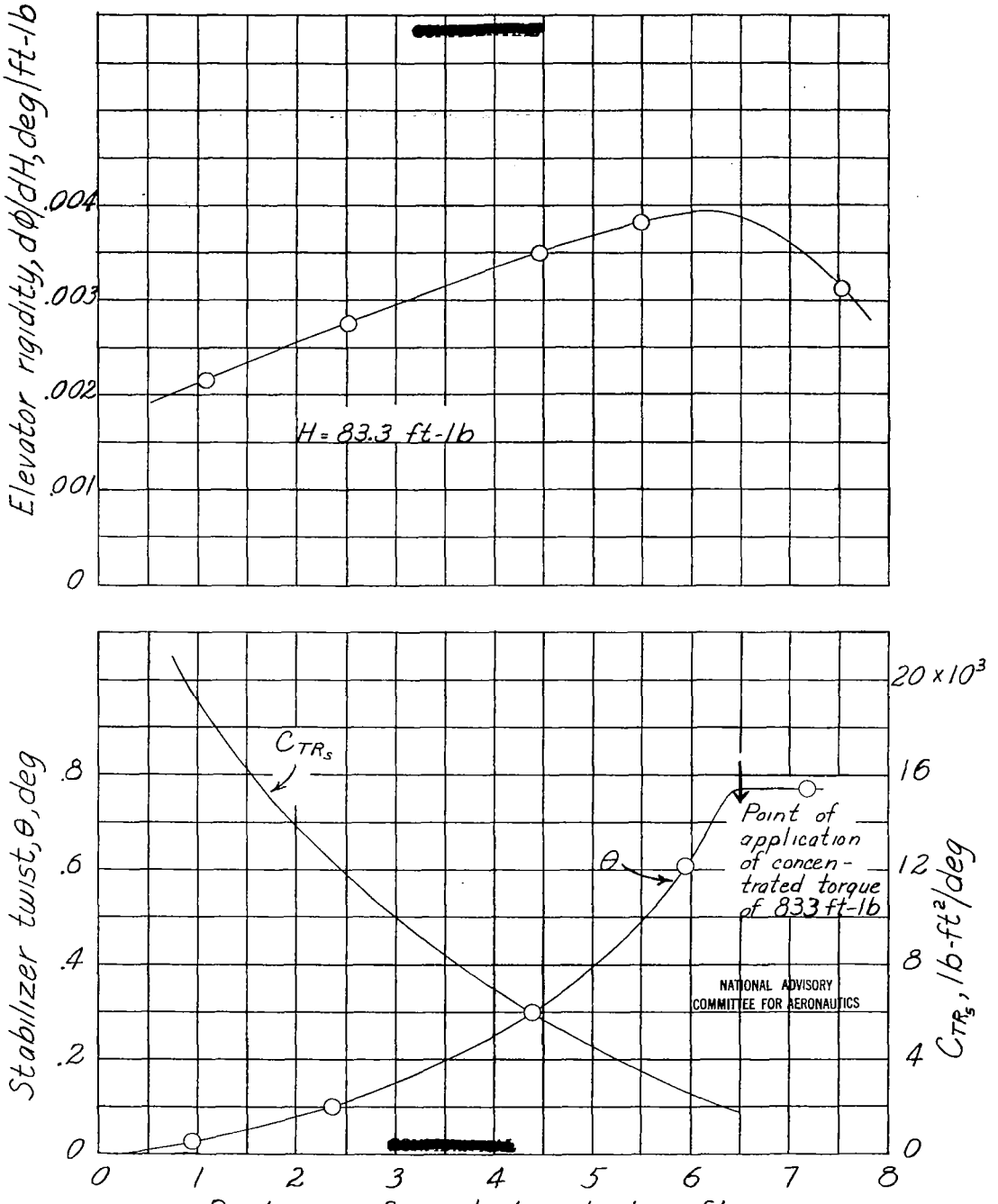

Figure 3.- Experimental data for flexibility of horizontal tail. Airplane A. Data from tests made by Langley Flight Research Division.

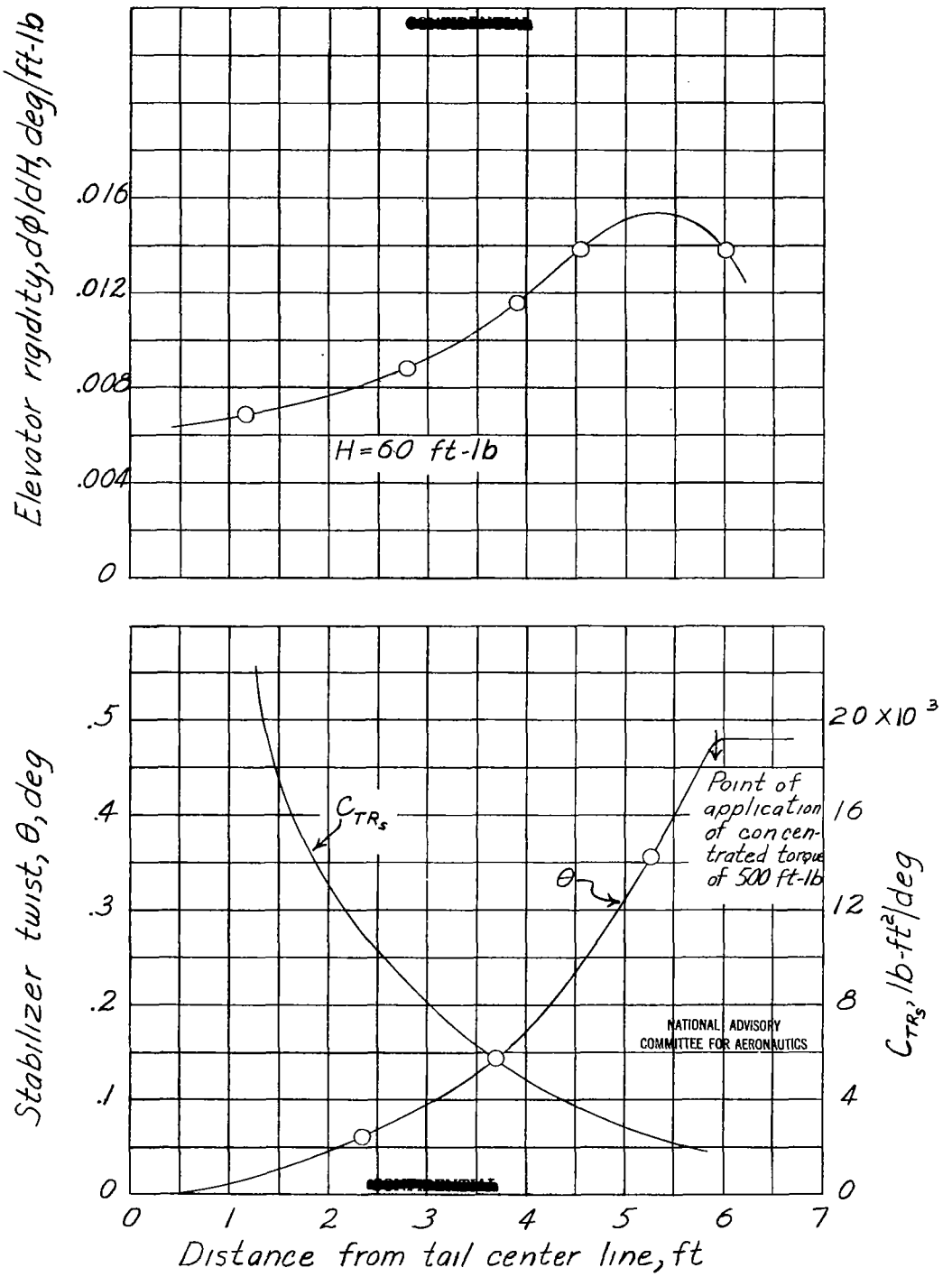

Figure 4.-Experimental data for flexibility of horizontal tail. Airplane B. Data from tests made by Langley Aircraft Loads Division.

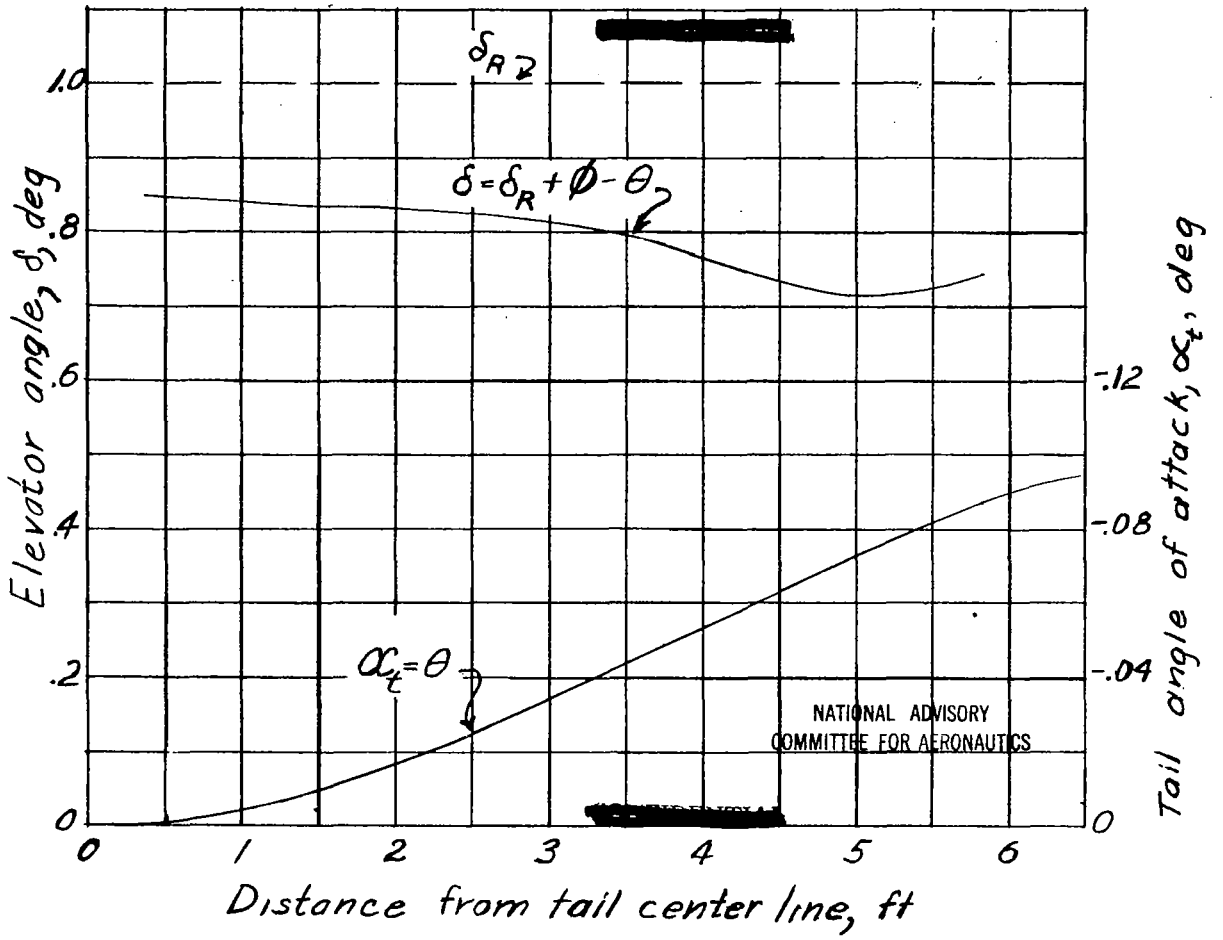

Figure 5.- Distribution of tail angle of attack and elevator deflection in a flexible tail resulting from an application of the elevator control equivalent to unit deflection for the assumed rigid tail. Airplane B; Mach number, 0.60 at sea level; $\delta_R = 1°$; $\alpha_{t_R} = 0°$.

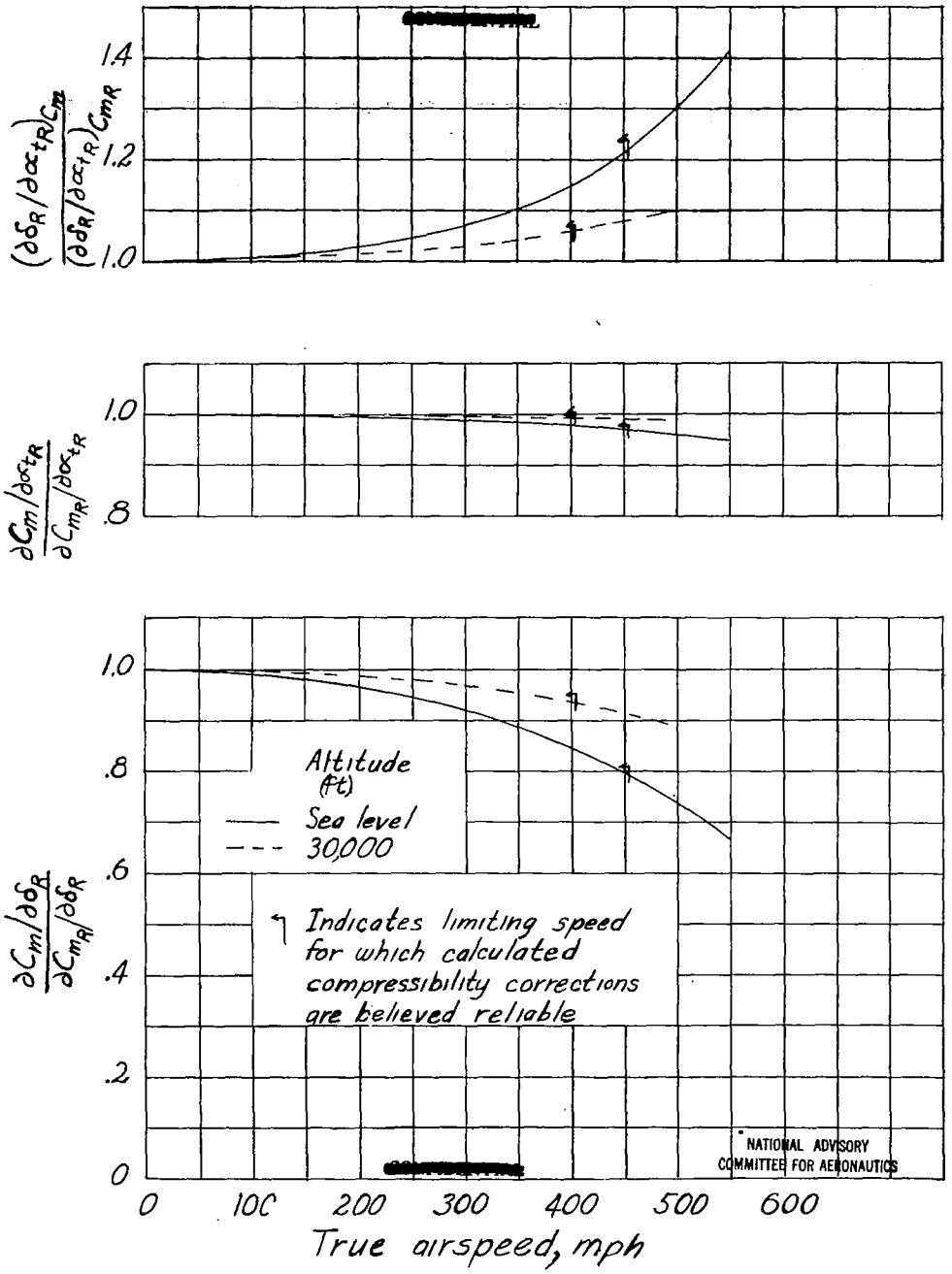

(a) Effectiveness parameters.

Figure 6.-Effect of horizontal-tail flexibility on longitudinal-control parameters. Airplane A.

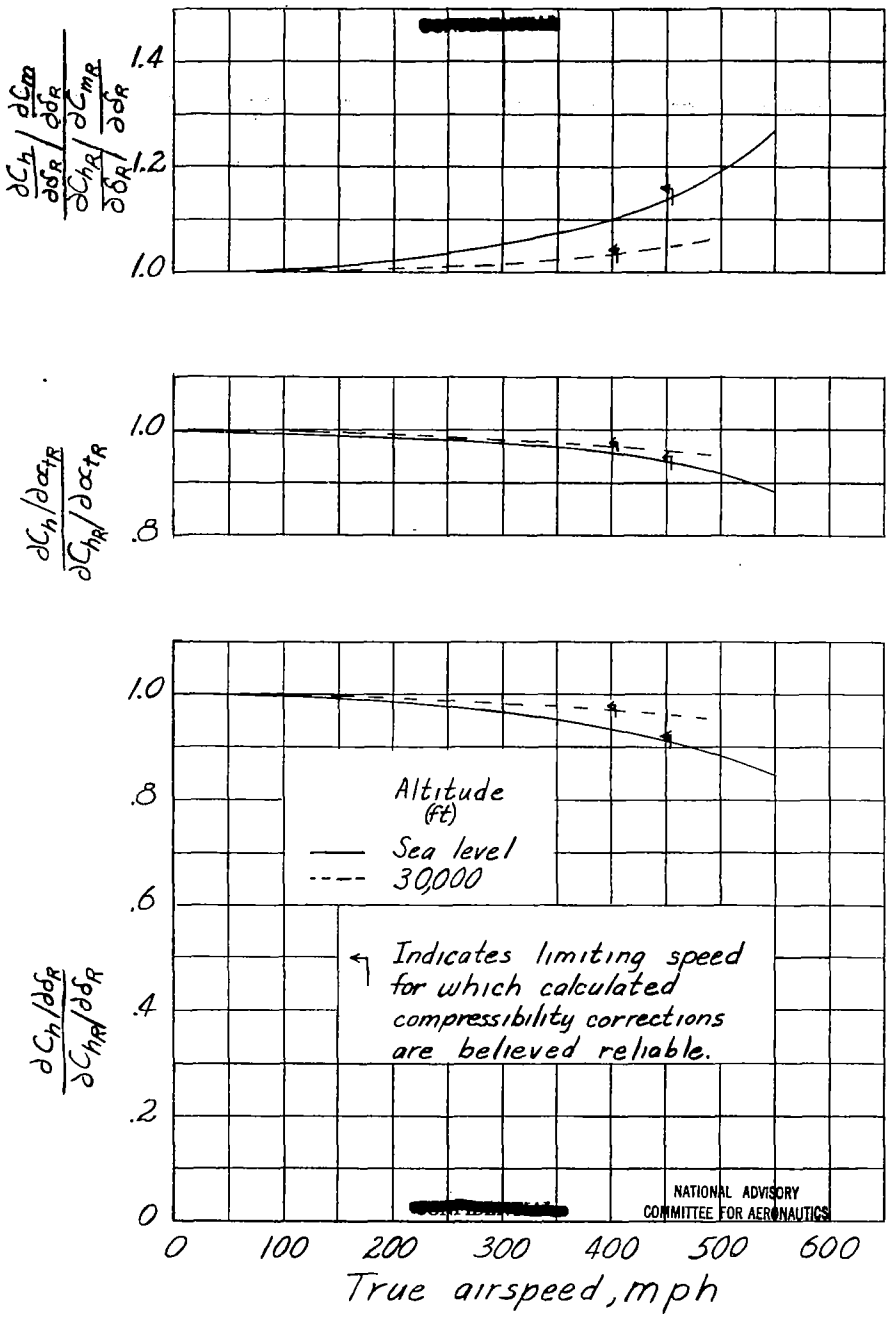

(b) Hinge-moment parameters.

Figure 6.-Concluded.

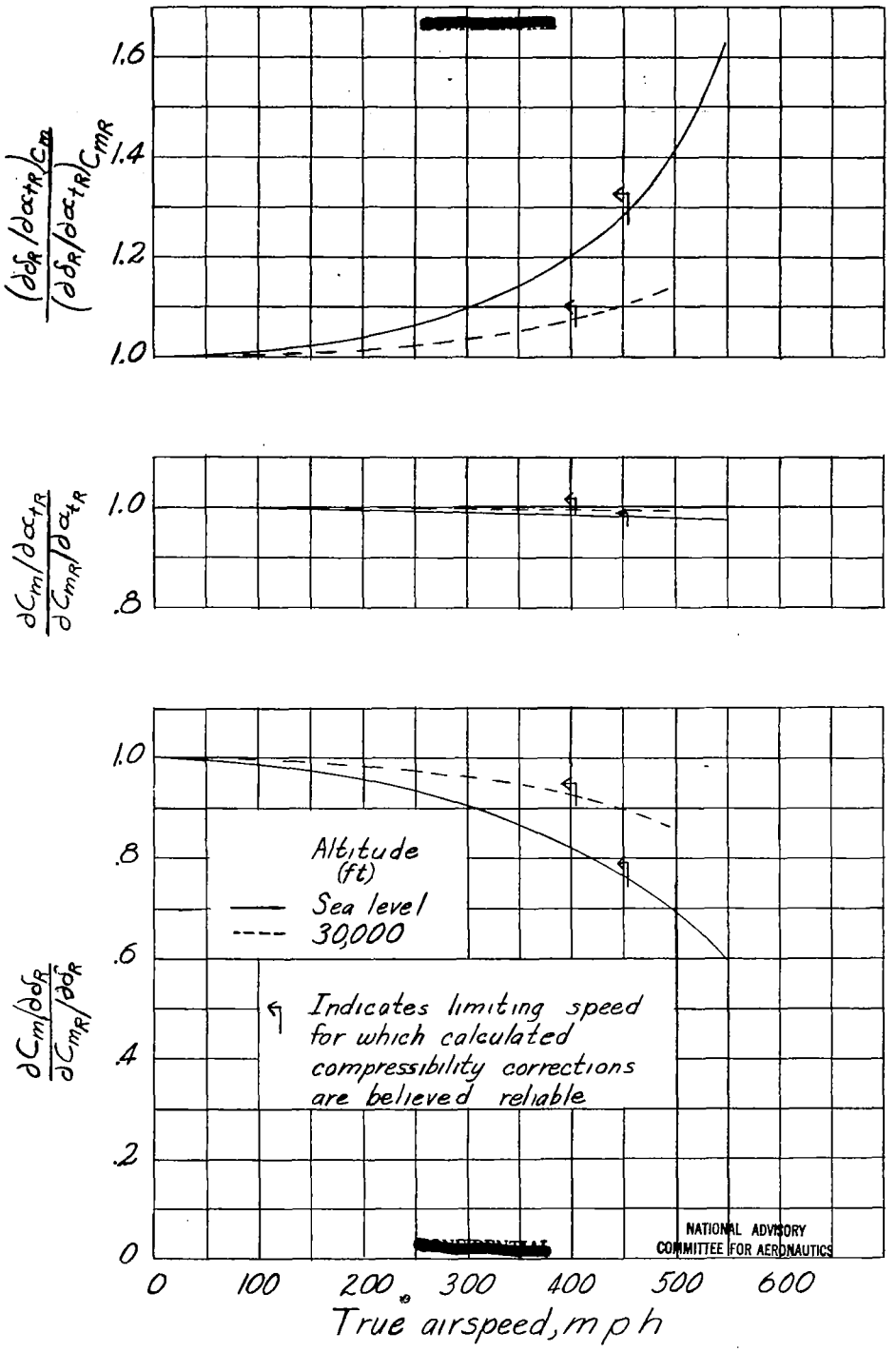

(a) Effectiveness parameters.

Figure 7.- Effect of horizontal-tail flexibility on longitudinal-control parameters. Airplane B.

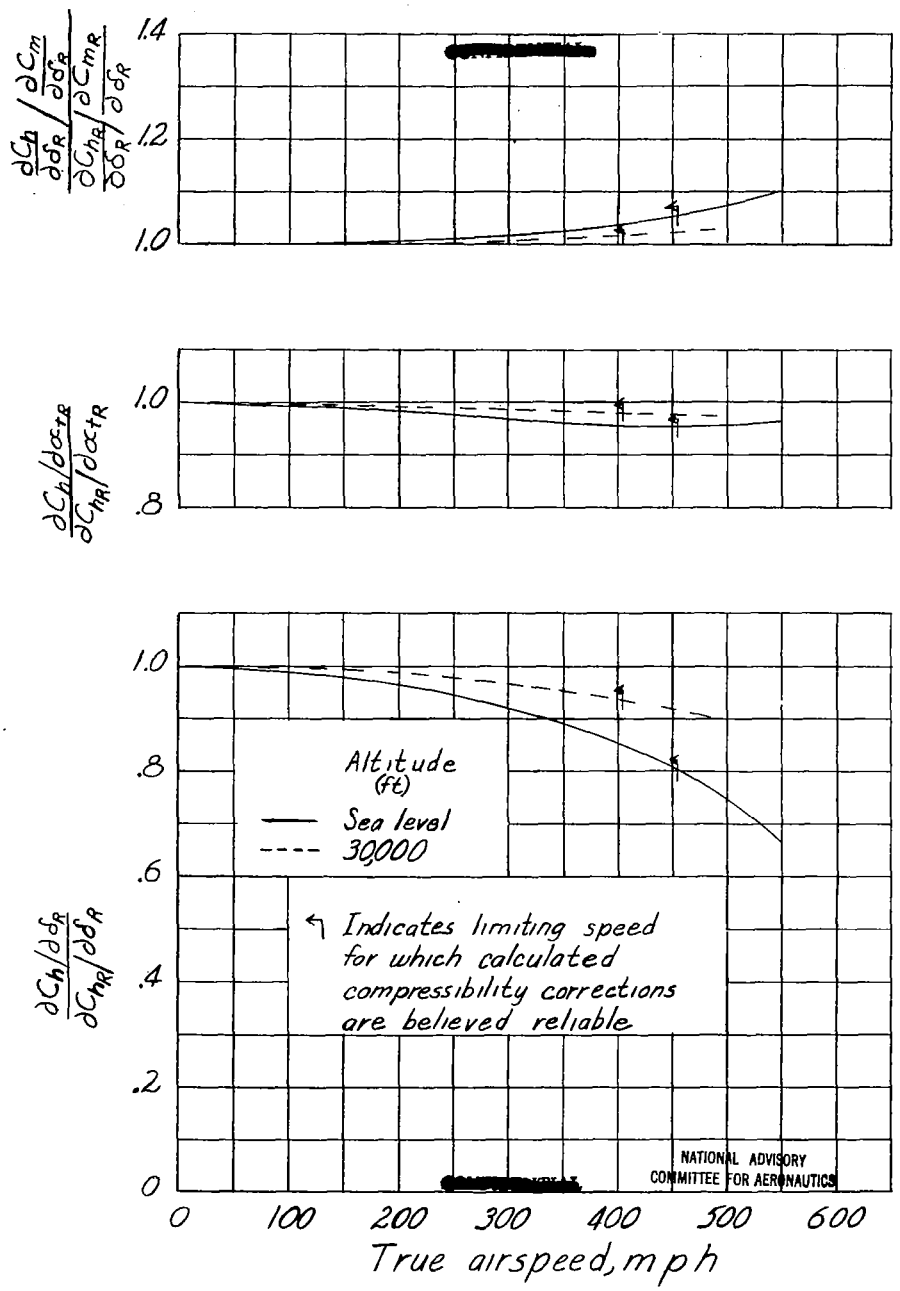

(b) Hinge-moment parameters.

Figure 7.- Concluded.

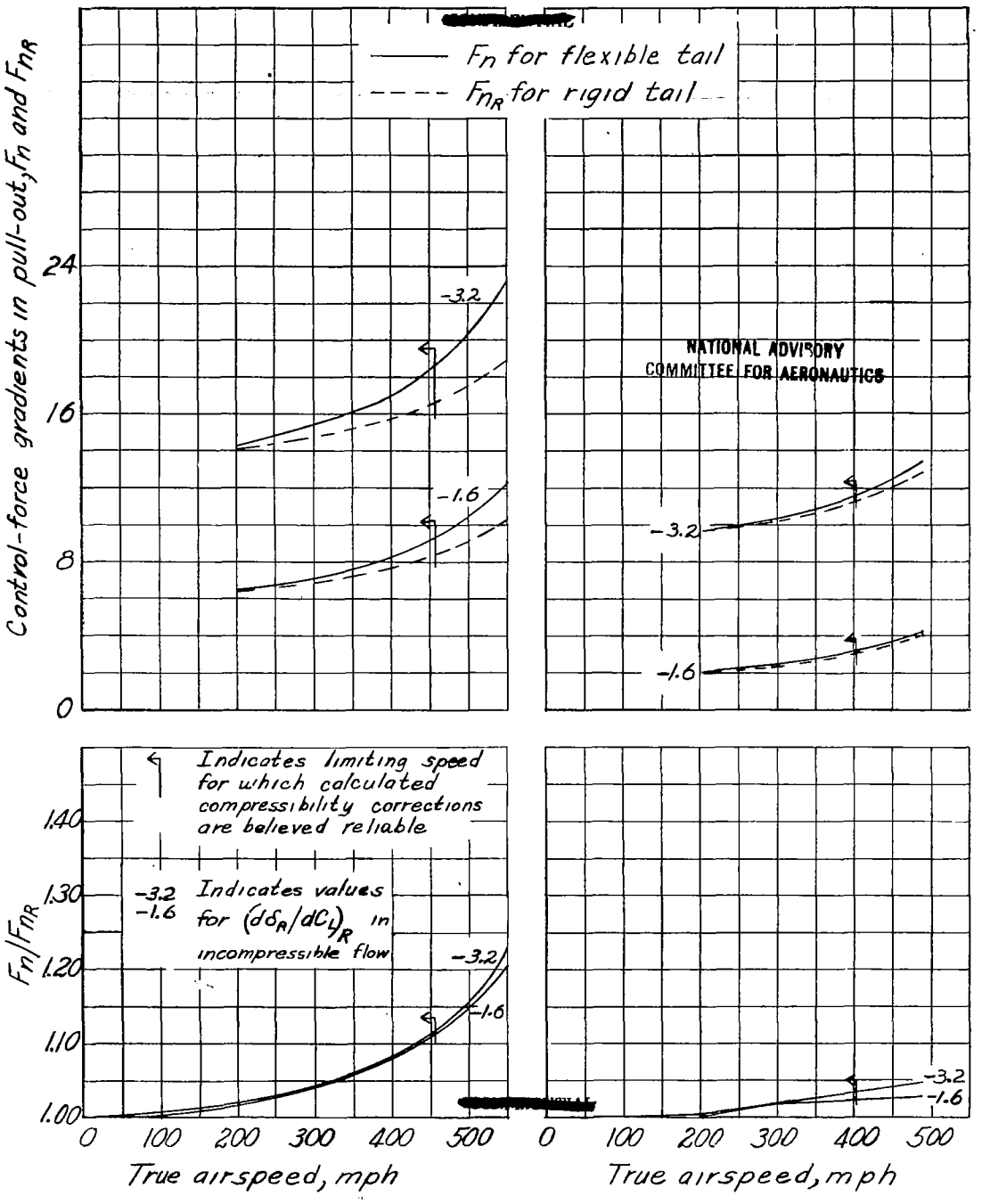

(a) At sea level. (b) At altitude of 30000 feet.

Figure 8.-Effect of horizontal-tail flexibility on elevator control-force gradients in recovery from dives. Airplane A.

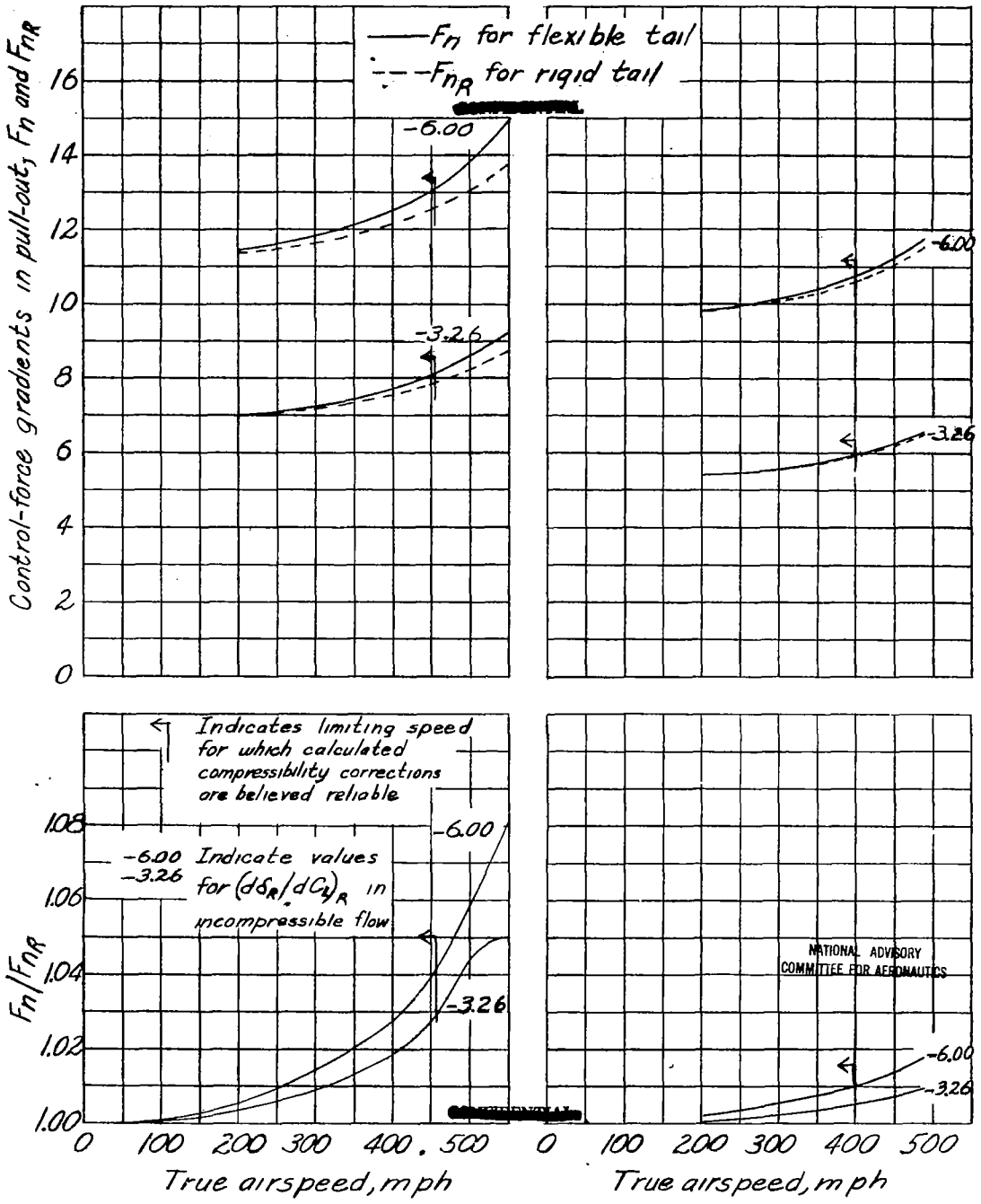

(a) At sea level. (b) At altitude of 30,000 feet.

Figure 9.- Effect of horizontal-tail flexibility on elevator control-force gradients in recovery from dive. Airplane B.